Neural Dysregulation During a Working Memory Task in Human Immunodeficiency Virus-Seropositive and Hepatitis C Coinfected Individuals

J.Z.K. Caldwell[1,2,3,4], **A. Gongvatana**[1,5], **B.A. Navia**[6], **L.H. Sweet**[1,7], **K. Tashima**[1,8], **M. Ding**[9], and **R.A. Cohen**[1,10]

[1] Department of Psychiatry and Human Behavior, Box G-BH, Brown University, Providence, RI 02912

[2] The Miriam Hospital, 164 Summit Avenue, Providence, RI 02906

[3] Marquette General Hospital, 580 W. College Ave, Marquette, MI 49855

[4] Michigan State University, Department of Psychiatry, East Lansing, MI 48824

[5] University of California, San Diego, 200 W. Arbor Drive #8231, San Diego, CA 92103-8231

[6] Department of Public Health, Infection Unit, Jaharis Family Center for Biomedical Research, Tufts Medical School, Boston MA 02111

[7] Department of Psychology, Psychology Building, 135 Baldwin Street, University of Georgia

[8] Lifespan/Tufts/Brown Center for AIDS Research, Brown University, Providence, RI 02912

[9] J. Crayton Pruitt Family Department of Biomedical Engineering, University of Florida, 1275 Center Drive, Biomedical Sciences Building J285, Gainesville, FL 32611

[10] Cognitive Aging and Memory Program, Clinical Translational and Research Program, University of Florida, 2004 Mowry Rd., Gainesville, FL 32611

Abstract

Cognitive and functional neural correlates of Human Immunodeficiency Virus (HIV) are only partially understood at present. Variability in neural response, which has been noted in the literature, may relate to clinical factors associated with HIV, including time since HIV diagnosis, (CD4) count and nadir, HIV viral load, and comorbid infectious processes, especially hepatitis C. The present investigation evaluated working memory-related functional neural activation in 26 HIV+ participants, 28 demographically matched HIV-seronegative individuals, and 8 HIV+ individuals with hepatitis C coinfection. Analyses examined impact of HIV infection duration, CD4 count and nadir, HIV viral load, and hepatitis C serostatus. Results showed that HIV-participants had fastest reaction times, and during the working memory task HIV+ participants

Corresponding Authors: Jessica Caldwell and Ron Cohen Jessica.kirklandcaldwell@mghs.edu; roncohen@ufl.edu Phone: 906-250-3568 Fax: 906-225-7456.

with hepatitis C coinfection showed strongest bias toward commission errors; however, signal detection (i.e., overall task performance) was equivalent across groups. Functional magnetic resonance imaging (FMRI) results showed HIV-related greater activation to an easier vigilance task and HIV-related lower activation to a more difficult working memory task, consistent with reduced cognitive reserve. Hepatitis C coinfection related to diffuse neural dysregulation. Correlational analyses suggested relationships of increasingly severe disease with poorer functioning in brain regions linked to error monitoring and attention regulation.

Keywords

HIV; hepatitis C; attention; working memory; functional MRI

Despite the advent of combination antiretroviral therapy (cART), many HIV-seropositive (HIV+) people exhibit neurocognitive deficits (Heaton et al. 2010). Further, in vivo neuroimaging has shown evidence of structural and functional brain abnormalities in cART-treated, medically stable cohorts (Chang et al. 2001; Chang et al. 2004; Ernst et al. 2009; Gongvatana et al. 2009; Ances et al. 2012). Functional underpinnings of HIV's deleterious effects on attention and working memory (Cohen et al. 2010b; Joska et al. 2010; Liner et al. 2010; Wendelken and Valcour 2012) remain of particular interest, as these basic cognitive skills play a role in higher-level cognition such as memory and executive function. In addition, success of attention and working memory depends on healthy function of brain regions and white matter tracts directly or indirectly impacted by HIV infection (for recent reviews, see (Burdo et al. 2010; Valcour et al. 2010).

In particular, structural or functional neural dysregulation in subcortical, frontal, and parietal regions may contribute to HIV+ individuals' attention and working memory deficits (e.g., (Clark and Cohen 2010). Research has shown HIV-related structural and metabolic abnormalities in subcortical regions including the basal ganglia (Beau M Ances, Ortega, Vaida, Heaps, & Paul, 2012; Beau M Ances et al., 2012; Becker et al., 2011; Cohen, Harezlak, Gongvatana, et al., 2010; Muller-Oehring, Schulte, Rosenbloom, Pfefferbaum, & Sullivan, 2010), and frontal and parietal cortex (Cohen et al. 2010a; Towgood et al. 2012; Gongvatana et al. 2013). Brain-wide gray and white matter changes have also been revealed (Thompson et al. 2005; Becker et al. 2012; Ragin et al. 2012).

Existing FMRI studies complement these volumetric and metabolic studies by suggesting inefficient neural processing in subcortical, frontal, and parietal networks in HIV+ individuals. For example, on tasks of visual attention, HIV+ participants show reduced activation in visual attention networks (i.e. prefrontal, dorsal parietal, and cerebellar regions), but increased compensatory activation elsewhere in the brain (Chang et al. 2004; Ernst et al. 2009). For progressively more complex visual attention tasks (i.e., tracking 4 rather than 1 moving targets), HIV+ individuals showed increased attention network response to the same task over a one-year interval, despite equivalent performance, whereas seronegative participants show less activation over the same interval. Working memory tasks have shown increased parietal activation for simple conditions in HIV+ individuals (i.e., 1-back tasks) (Chang et al. 2001) and increased frontal activity, especially for more

complex conditions (i.e., 2-back tasks) (Ernst et al. 2002). In addition, although HIV+ individuals show greater magnitude neural activation for more complex relative to simpler tasks in prefrontal and parietal cortices, this relative increase is significantly smaller than that seen in HIV-seronegative participants (Tomasi et al. 2006). This finding, which has been referred to as reduced dynamic range of activation, may suggest reduced cognitive reserve due to inefficient processing in HIV+ individuals, similar to what has been suggested in individuals with other CNS-impacting disorders such as multiple sclerosis (Chang et al. 2001; Penner et al. 2003; Sweet et al. 2006).

Importantly, FMRI investigations have also indicated HIV+ participants have less stability in the blood oxygen level dependent (BOLD) response to cognitive challenge—or in other words, more variable neural activation during cognitive tasks (Ances et al. 2011). This reduced stability has been shown to relate to HIV disease severity markers, such as presence of HIV-associated neurocognitive disorders (i.e., HAND) (Chang et al. 2013), effectiveness of individual treatment (Ances et al. 2008), and presence of cART (Chang et al. 2008). Variability may also explain some discordance in FMRI investigation results within HIV+ individuals. These findings, along with known relationships of more severe HIV disease with more advanced cognitive impairment or structural brain changes (Cohen et al. 2010b; Sun et al. 2010; Ellis et al. 2011; Devlin et al. 2012; Crum-Cianflone et al. 2013) underscore the importance of examining the contribution of clinical factors to alteration in functional MRI responses.

HCV coinfection is another clinical factor that may impact neural function in HIV+ individuals. Up to 25% of HIV+ individuals are coinfected with hepatitis C (HCV) (Kim et al. 2013), and studies within our research group and others suggest deleterious impact of comorbid HCV on cognition (Devlin et al. 2012; Rempel et al. 2013; Sun et al. 2013) and cytokine predictors of cognition (Cohen et al. 2011). Evidence has accumulated for impact of HCV coinfection on brain structure (Jernigan et al. 2011; Pfefferbaum et al. 2012) and brain metabolism (Forton et al. 2001; Taylor et al. 2004; Winston et al. 2010; Garvey et al. 2012). However, functional neural consequences of HIV/HCV coinfection during active tasks have not been explored.

Previous research has provided evidence for the impact of HIV on attention and working memory, with functional MRI tasks suggesting reduced activation due to low cognitive reserve in task-related regions and reliance on compensatory activation in additional neural regions. However, studies to date leave open questions regarding impact of HIV-related clinical factors, including time since HIV diagnosis, CD4 count and nadir, and viral load. Moreover, no active task FMRI studies have directly addressed the impact of HCV coinfection. Thus, the present study aimed to characterize the impact of HIV infection and HIV disease makers (i.e., hepatitis C coinfection, CD4 count and nadir, plasma viral load) on neural response to a working memory paradigm. We hypothesized that HIV+ individuals would show increased prefrontal cortical activation for a 2-back working memory task, as well as a reduced neural response to the working memory task, after accounting for response during the control task (i.e., reduced dynamic range), particularly in regions shown to have reduced dynamic range in previous investigations, such as prefrontal and parietal regions. We expected individuals with longer time since HIV diagnosis, detectable plasma viral load,

and lower nadir and current CD4 levels to show more dysregulation of neural activation. We further hypothesized that HIV/HCV coinfected individuals would show an exaggeration of the functional dysregulation in HIV+ individuals.

Method

Participants

Participants were 85 adults recruited from The Miriam Hospital Immunology Center as part of an NIH-sponsored study of HIV-associated brain dysfunction. Institutional review boards approved the study and informed consent was obtained from each participant before enrollment. All participants underwent a neurological examination and thorough medical history assessment. HIV infection was documented by enzyme-linked immunosorbent assay (ELISA) and confirmed by Western blot. Active HCV infection was defined as positive anti-HCV by ELISA and positive qualitative HCV RNA by polymerase chain reaction.

Exclusion criteria included head injury with loss of consciousness of greater than 10 minutes; neurological complications including dementia, seizure, stroke, and opportunistic brain infection; severe psychiatric illness; and substance dependence during the 6 months prior to the baseline evaluation or positive urine toxicology for cocaine, opiates, stimulants, or sedatives at the time of the baseline evaluation[1]. Further exclusions were made due to lack of functional MRI data, (1 participant), scanner artifact or excessive head motion (3 participants), failure to perform the N-back task to criterion level (i.e., <75% correct 0-back trials or failure to follow instructions; 5 participants), and combined head motion and performance issues (9 participants). After all exclusions, the total sample size included in the present analysis was 62.

Basic demographic characteristics for our sample are as follows. Twenty-six participants were female. Participants included 28 HIV seronegative individuals, 26 HIV+ individuals, and 8 HIV/HCV seropositive individuals. Average participant age was 45 years. For HIV+ and HIV/HCV seropositive participants, the average amount of time since diagnosis of HIV infection was 7.6 years. For these same individuals, average current CD4 count was 550, average CD4 nadir was 201, and average HIV viral load was 30,375. The majority of HIV+ and HIV/HCV seropositive participants were on cART treatment at the time of the fMRI scan (i.e., 79%). When directly comparing HIV seronegative, HIV+, and HIV/HCV seropositive groups, there were no significant differences in age, gender, or race (Table 1); however, HIV/HCV coinfected participants showed a trend toward lower educational attainment than either HIV seronegative or HIV+ participants ($\chi^2 = 4.657$; p = 0.097). Within HIV+ participants, those coinfected with HCV did not differ from the larger HIV+ group in terms of time since HIV diagnosis, current CD4 value, CD4 nadir, current viral load

---

[1]Participants who met substance dependence criteria at later time points (i.e., 12 or 24-month visits) were not excluded from participation. For time points most proximal to participant MRI scan, 44% of individuals qualified for lifetime diagnosis of alcohol dependence (3% proximal to MRI; no significant differences between clinical groups). Lifetime cocaine dependence was met in 42% of participants (5% proximal to MRI). Kruskall-Wallis tests showed significant group differences for endorsement of lifetime ($\chi^2 = 10.143$, p = 0.006) and MRI-proximal cocaine dependence ($\chi^2 = 8.345$; p = 0.015; highest rates in HIV/HCV coinfected participants). Lifetime narcotic dependence was met in 15% of participants (2% proximal to MRI), with significant differences among clinical groups for lifetime ($\chi^2 = 22.463$, p < 0.001; highest rates in HIV/HCV coinfected participants), but not MRI-proximal dependence.

detectability, or current cART treatment (Table 1). See Table 1 for additional participant demographic information.

Task

We employed a verbal N-back FMRI paradigm (Owen et al. 2005) during which a series of consonant letters was visually presented. Participants responded either Yes or No using a response button box following the presentation of each letter, indicating whether it is the same as or different from the letter presented N items earlier. Each letter was presented for 500ms with a 2500ms inter-stimulus interval. Uppercase and lowercase letters were randomly presented. 0-back and 2-back conditions were used in this experiment. Data were acquired in two separate task runs. Each run consisted of alternating blocks of 3 36s 0-back trials, 3 45s 2-back trials, and 3 30s resting block during which a stationary cross was presented; including instruction time, total task length was 12 minutes.

Statistical Analysis

Performance on the 0-back and 2-back tasks was indexed by percentage correct target and total trials, A' (a nonparametric measure of signal detection that takes into account both omission and commission errors) (Snodgrass and Corwin 1988), mean reaction time (RT), and reaction time variability (Simmonds et al. 2007). Due to differing sample sizes and non-normal distribution of several variables, nonparametric Mann-Whitney or Kruskall-Wallis tests were used to compare demographic, clinical, substance use, and performance data for HIV+ and HIV-seronegative individuals, as well as HIV+ and HIV/HCV-seropositive individuals.

FMRI Data Acquisition

Whole-brain, echoplanar BOLD FMRI images were acquired in 42 interleaved axial 3mm slices (TR=2500ms, volumes=147, TE=28ms, FOV=192×192 mm, matrix=64×64) on a Siemens 3 Tesla TRIM TRIO magnet (Siemens Corporation 2013).

FMRI Analysis

Analyses were completed primarily using FEAT (FMRI Expert Analysis Tool) Version 5.98, part of FSL (FMRIB's Software Library, www.fmrib.ox.ac.uk/fsl). Cortical reconstruction and removal of non-brain tissue were performed with the Freesurfer image analysis suite (http://surfer.nmr.mgh.harvard.edu/; Segonne et al., 2004). Registration to high resolution structural and standard space images was carried out using FLIRT (Jenkinson and Smith 2001; Jenkinson et al. 2002) and further refined using FNIRT nonlinear registration (Andersson et al. 2007; Andersson and Smith 2007).

Individual subject analysis—After reconstruction, functional data for the two task runs for each subject were entered into separate first-level mixed-effects analyses in FEAT. Data were motion corrected, smoothed (FWHM=6m), and high-pass temporal filtered (140s). Film prewhitening was applied. Task instructions, 0-back, and 2-back trials, as well as their temporal derivatives, were included in the model. A double-gamma hemodynamic response function model was employed. Outlying data due to subject head motion were included as

confound variables using fsl_motion_outliers. Contrasts of interest at the run level included activation to 0-back trials and 2-back trials relative to rest, as well as differences between these conditions (i.e., 0-back > 2-back; 2-back > 0-back). Data passing quality control thresholds were passed on to second-level fixed-effects GLMs averaging within subject, across runs. Second-level contrasts were identical to first-level contrasts.

Group analysis—Third-level group analysis employed FSL randomise (Bullmore et al. 1999; Nichols and Holmes 2002; Hayasaka and Nichols 2004), a permutation-based method for GLM analysis. For data display, all figures were created using MRIcron; text was overlaid on images using Adobe Photoshop.

The first aim of the group analysis was to examine group activation (i.e., HIV+, HIV-seronegative, and HIV/HCV coinfected) to each of the two task conditions (i.e., 0-back vs. rest; 2-back vs. rest) and for the contrast of the two task conditions (2-back > 0-back). This latter contrast was calculated as a measure of dynamic range in neural activation between the more difficult and an easier tasks. A second and related aim was to contrast neural activation differences between each of the three groups (i.e., HIV+, HIV-seronegative, and HIV/HCV coinfected) on all task conditions (i.e., 0-back vs. rest; 2-back vs. rest; 2-back > 0-back).

Based on these aims, three GLMs were run, modeling 0-back vs. rest, 2-back vs. rest, and 2-back > 0-back, respectively. Within each GLM, contrasts of interest were main effects for each clinical group (positive and negative activations for HIV+, HIV-seronegative, and HIV/HCV coinfected), and direct comparisons among the diagnostic groups. Probability of gray matter was entered into the matrix as a voxelwise covariate to control for potentially confounding anatomical variation (See Oakes et al. 2007). Family-wise error rates of $p < 0.01$ or lower were employed (See tables for exact values).

Examination of additional clinical factors—Additional aims of the study were to examine the potential relationship of clinical disease factors with neural activation in HIV+ and HIV/HCV coinfected participants. For this analysis, time since HIV diagnosis, CD4 and CD4 nadir were demeaned and individual subject scores were entered into separate group-level GLMs in FSL FEAT. Again, separate GLMs were run for 0-back vs. rest, 2-back vs. rest, and 2-back > 0-back. Contrasts of interest included main effects for group (i.e., HIV+; HCV coinfected) and main effects for clinical factors. In each GLM, outlier detection was used to eliminate effects of extreme data points and gray matter probability was included as a voxelwise confound covariate. Analyses were corrected for multiple comparisons using voxelwise thresholds of a minimum $z > 2.464$, and cluster probability thresholds based on Gaussian Random Field Theory of $p < .05$. Given the relatively smaller sample size for these analyses (N = 34), as well as the relatively small literature examining continuous HIV clinical factors with working memory response, thresholds were then relaxed to examine covariate trends for further study.

Impact of current HIV plasma viral load detectability was examined by grouping all individuals with HIV (including those with HCV coinfection) by plasma viral load detectability. As above, permutation-based GLM analyses were run for each condition of

interest (i.e., 0-back vs. rest, 2-back vs. rest, and 2-back > 0-back); group main effects and contrasts of these two clinical groups were examined. Probability of gray matter was entered into the matrix as a voxelwise covariate. Family-wise error rate of $p < 0.01$ or lower were employed (See supplementary tables for exact values). As with covariate analyses, thresholds were subsequently relaxed to examine covariate trends.

Results

N-Back FMRI Response By Clinical Group

The first analytical goal was to examine activation in all three clinical groups (i.e., HIV+, HIV-seronegative, and HIV/HCV coinfected) for each of the two task conditions (i.e., 0-back, 2-back) and the contrast of these two conditions (2-back > 0back), which was calculated as an assessment of dynamic range of neural activation between an easier task and a more challenging task. Regions of significant neural activation by task condition, for each clinical group, are provided in Table 3.

0-back task—Activation for the 0-back task was observed for all groups in regions consistent with previous literature, including left motor cortex, left parietal regions, and bilateral supplementary motor area, frontal, occipital, and cerebellar regions (See Table 3).

2-back task—For the 2-back task, activation was observed in similar regions as observed during the 0-back task for all clinical groups. HIV-seronegative participants additionally showed activation in right superior temporal and right parietal regions, while HIV+ participants showed additional activation of right insula and basal ganglia, and HIV/HCV coinfected participants showed additional activation in left inferior temporal regions and bilateral basal ganglia (See Table 3).

2-back > 0-back—When the 2-back and 0-back tasks were directly compared as an assessment of dynamic range of neural activation, all three clinical groups showed greater activity in bilateral parietal, frontal, and supplementary motor areas. HIV-seronegative participants also showed greater activation in bilateral cerebellum and inferior temporal regions. HIV+ individuals also showed greater bilateral cerebellar activation. Both HIV+ and HIV/HCV coinfected individuals also showed greater bilateral precuneus and basal ganglia activation (See Table 3).

N-Back FMRI Activation Differences Between Clinical Groups

The second analytical goal was to assess N-Back FMRI response differences when comparing clinical groups (i.e., HIV+, HIV-seronegative, and HIV/HCV coinfected). Significant between-group differences in neural activation, by task condition, are presented in Table 4.

0-back task—In a direct comparison, HIV+ and HIV-seronegative participants did not show differences in 0-back activation. HIV/HCV coinfected participants showed greater 0-back activation in bilateral cerebellar and occipital regions than HIV-seronegative participants (See Table 4).

2-back task—Direct comparisons of clinical groups again showed no significant activation differences between HIV+ and HIV-seronegative individuals. HIV/HCV coinfected participants showed greater activation compared to HIV-seronegative participants in bilateral frontal regions, cerebellum, and basal ganglia; as well as left supplementary motor, and right postcentral and angular gyrus (See Table 4 and Figure 1A). HIV/HCV coinfected participants showed significantly greater 2-back task activation compared to HIV+ participants in bilateral cerebellum and right frontal, precentral, precuneus, and occipital regions (See Table 4 and Figure 1A).

2-back > 0-back—In a direct contrast of HIV + and HIV-seronegative participants, HIV-seronegative individuals showed greater dynamic range (i.e., greater 2-back compared to 0-back activation) in right inferior temporal regions, bilateral thalamus, and bilateral occipital and parietal cortices (See Table 4 and Figure 1B).

Additional Clinical Factors and Neural Activation

Time since HIV diagnosis—In HIV+ participants, longer time since HIV diagnosis was associated with greater 0-back task activation relative to rest in the bilateral basal ganglia (See Table 5). A trend-level relationship was revealed for longer estimated HIV duration with broadly greater activation during both tasks, with regions of note including precuneus, angular gyrus, posterior cingulate, occipital, temporal, and frontal regions (See Table 5). Within HIV/HCV coinfected participants, positive trends were observed between time since diagnosis and greater 2-back task activation in the left hippocampus and temporal regions. Positive trends were also observed for HIV/HCV coinfected participants' time since diagnosis and activation in several regions for the 2-back > 0-back condition.

CD4 nadir—CD4 nadir in HIV+ individuals was associated with greater 2-back task activation relative to rest in right inferior frontal cortex and bilateral cerebellum and occipital regions (Table 5). Several trend-level relationships were observed, including negative trends relating CD4 nadir with 0-back activation relative to rest in the posterior cingulate in HIV+ individuals, and negative trends relating CD4 nadir with bilateral basal ganglia and cerebellum response in HIV/HCV coinfected individuals (Table 5).

Current CD4 count—For HIV+ participants, higher current CD4 count was associated with significantly greater 0-back relative to rest responses in the orbitofrontal cortex, greater 2-back relative to rest responses in right pre- and post-central gyrus (See Table 5), and lower responses in bilateral occipital cortex for the 2-back > 0-back condition. HIV/HCV coinfected participants showed a negative association of current CD4 with 0-back responses in right occipital regions, and a positive association with 2-back responses in the right anterior cingulate (See Table 5). Trend-level negative associations were observed for CD4 count with 0-back task activation in the bilateral anterior cingulate and medial frontal gyrus for HIV+ participants. Additional trends included positive associations of CD4 count with 0-back task activation in the left middle and superior temporal gyri and bilateral anterior cingulate cortex (ACC'; 2-back task activation in right occipital, left inferior frontal, and bilateral basal ganglia; and 2-back > 0-back task activation in left frontal regions for HIV/HCV coinfected participants.

Detectable viral load—Trends only were observed for viral load analyses. Specifically, HIV+ participants with detectable viral load showed a trend toward greater 0-back task activation relative to rest in the bilateral cerebellum, as well as broad and diffuse activation across the bilateral frontal cortex, precuneus, and posterior cingulate (See Table 6). Detectable viral load was also associated with trends toward greater 2-back activation relative to rest in bilateral orbitofrontal and left basal ganglia and temporal cortex (See Table 6), and greater 2-back > 0-back increases in a diffuse network including bilateral temporal, orbitofrontal and subgenual cingulate cortices. Those with undetectable viral load showed trends toward greater 0-back task activation in left superior parietal and post central regions; greater 2-back activation in left superior parietal and lateral occipital cortex; and greater 2-back > 0-back increases in a diffuse network including but not limited to the right ACC and superior frontal regions.

N-Back Task Performance

See Table 2 for full details of performance results.

0-Back—Kruskall-Wallis tests showed no significant group differences in 0-back reaction time variability, bias (B'), or signal detection (A'). However, groups differed significantly in 0-back reaction time ($\chi^2 = 6.932$, p = 0.031; Table 2), with HIV-seronegative participants having fastest reaction times.

2-back—Kruskall-Wallis tests showed no significant group differences in 2-back reaction time variability or signal detection; however, groups differed significantly in terms of 2-back bias ($\chi^2 = 7.532$, p = 0.023) and reaction time ($\chi^2 = 8.764$, p = 0.013; Table 2). Again, HIV-seronegative participants had fastest reaction times. HIV/HCV coinfected individuals showed a strong positive bias (i.e., tendency to make a false positive error), while HIV-seronegative participants had a mild positive bias (i.e., tendency to make a false positive error) and HIV+ participants had a mild negative bias.

Discussion

The results of the present study extend previous findings that have demonstrated functional brain disturbances on tasks requiring working memory in people infected with HIV (Chang et al. 2001; Ernst et al. 2002; Chang et al. 2004; Ernst et al. 2009). The current 2-back task requires working memory along with sustained and focused attention. In contrast, the 0-back task requires sustained attention and vigilance, but does not have significant working memory demands. Here, HIV seropositive participants showed less difference in brain activation between the 2-back and 0-back tasks, compared to the seronegative participants. Specifically, people with HIV had greater activation on the simpler sustained attention task (0-back), but less activation on the working memory task (2-back). This finding is consistent with previous work that suggests HIV affects the brain by causing a reduction in dynamic range in response to cognitive challenge (Tomasi et al. 2006). Reduced dynamic range is consistent with the hypothesis that even in the post-cART era, HIV continues to affect brain functioning (Ernst et al. 2009; Clark and Cohen 2010), and in particular results in reduced cognitive reserve that requires HIV seropositive individuals to expend more cognitive

resources on simpler tasks. In the present study, a reduction in functional range was observed despite comparable task performance, with the exception of slower reaction time for those with HIV.

The present investigation also showed that several clinical factors impact neural activation in the context of HIV infection. In particular, hepatitis C (HCV), which has been linked to poorer cognitive outcomes in previous work by our lab (Devlin et al. 2012) emerged as an important clinical variable. Individuals with HIV and HCV coinfection showed a broad and diffuse pattern of greater neural activation than HIV negative participants on both the 0-back and 2-back working memory tasks. When compared to HIV+ participants, coinfected individuals again showed diffuse, greater neural activation during the working memory task. The pattern of this latter contrast, which reflects the specific effect of hepatitis C, was not entirely straightforward, and some caution must be used in interpretation due to the relatively smaller size of our HIV/HCV positive sample. However, results suggest broadly increased activation, including within regions overlapping with the working memory network, which may suggest that comorbid HCV does not have a simple additive impact over HIV serostatus in reducing of cognitive reserve, as we had predicted. In addition, HIV/HCV coinfected participants showed greater working memory-related activation in task-irrelevant regions, including some—like the angular gyrus—which are typically associated with self-directed rather than task-directed attention (Raichle et al. 2001; Gusnard et al. 2001). Again, functional differences were observed despite comparable performance on the task, perhaps due to a behavioral response bias whereby the HIV/HCV coinfected participants were more likely to make false positive errors. Such as response bias would be consistent with expectations for people with frontal lobe dysfunction affecting inhibitory control.

Other clinical factors tested, including detectability of HIV virus, time since HIV diagnosis, CD4 nadir, current CD4 count, and viral load detectability, also related to task activation. Results revealed that longer time since HIV diagnosis related to greater working memory activation in occipital cortex and the precuneus, a region involved in self-directed attention. In contrast, higher current CD4 count was associated with less activation in regions associated with self-directed thought, and with greater activation in regions associated with error detection. Somewhat less clear positive associations emerged between CD4 nadir and cerebellar, occipital, and inferior frontal neural activation during the working memory task. In addition, trend-level results suggested a positive relationship of viral load detectability and time since HIV diagnosis with diffuse activation in a network of regions that included several important for self-directed attention: the precuneus, posterior cingulate, and frontal cortex. Greater CD4 nadir showed trend-level associations with lower activity in regions important for self-directed attention, and greater activity in regions important for error detection and monitoring. Finally, analyses revealed a complex pattern of trend-level associations of current CD4 count with frontal cortical activation. These clinical factor results, while preliminary, warrant follow up in larger samples.

The present finding that effect differences between the HIV seropositive and seronegative groups were primarily observed as a function of the dynamic range of cortical activation with increasing task demand suggests the effects of HIV on the brain in the post-cART era

may not be revealed by examination of brain response during individual tasks (e.g., attention/vigilance and working memory) in isolation, or at a single level of difficulty. It also supports previous work showing that HIV+ individuals' neural dysregulation is not limited to more difficult tasks (Chang et al. 2001; Ernst et al. 2002; Chang et al. 2004; Ernst et al. 2009), but that impairment—or need for additional cognitive reserve—is evident in basic functions, such as attention. As intact attention is necessary for successful engagement of more complex cognitive functions such as working memory and executive functioning, continued work on functional neural correlates of attention in HIV, using sensitive measures, is needed.

In contrast to the HIV effect, the present study revealed a more complex picture regarding the effects of specific HIV-associated clinical factors. HIV/HCV coinfected individuals and those with current detectable viral load exhibited a more diffuse pattern of activation, including in brain regions not normally associated with working memory. This suggests that coinfected participants and those with most active disease experienced more diffuse neural dysregulation, a finding consistent with reduced neural efficiency in the face of comorbid or severe disease. HIV/HCV coinfected individuals and those with detectable HIV viral load also showed greater activity in some regions important for self-directed attention. Time since HIV diagnosis, lower CD4 nadir, and lower current CD4 count also related to increased activity in these regions. Areas such as the posterior cingulate and angular gyrus are traditionally associated with default network—a network hypothesized to be important for self-directed attention, which is typically not active during cognitive tasks. Coupled with findings of increased activation in error-monitoring regions in those with less severe CD4 nadir, the present results suggest a simultaneous failure of self- and other- directed attention in more severe disease. If future work replicates this finding in larger HIV/HCV comorbid samples and those with participants who have detectable viral load, it may suggest that part of the impact of comorbidity and acute disease on cognitive functions (Devlin et al. 2012) is via not only failure of task-relevant attention networks and potentially compensatory activation in task-unrelated regions, but also via dysregulation within self-directed attention networks that are traditionally functionally decoupled from active-task relevant networks (Fox et al. 2009).

Relative to previous work, the present study is unique in that it includes a large sample and examines several clinical variables in the context of HIV infection. The present study also adds to the literature in its control for gray matter probability at any given functional voxel; we can confidently say the present results are not solely a reflection of underlying disease-related structural neural changes. In addition, this study lends further support to previous work from our group and others that shows continued impact of HIV in the post-cART era, including impact on cognition (Clark and Cohen 2010; Devlin et al. 2012), and brain structure and function (Letendre et al. 2009; Cohen et al. 2010b; Clark and Cohen 2010; Gongvatana et al. 2013).

Limitations of the present study include a relatively small sample of HIV/HCV coinfected individuals, the exploratory nature of some analyses with clinical factors, and loss of a number of participants due to poor performance and head motion during scanning. Future studies of larger samples of people with HCV and HIV/HCV co-infection are needed to

Author Manuscript

Author Manuscript

Author Manuscript

Author Manuscript

confirm and expand our understanding of the impact of HCV on functional brain activation. More work is also required to ascertain relationship of HIV clinical factors with neural function, especially in light of the fact that several of these factors are derived from patient self-report (i.e., time of diagnosis), and may have inherent reporter error. Finally, in excluding participants who did not meet a standard performance threshold, we ensured that we are examining neural activation in participants who are attempting the task and showing some degree of ability to complete the task; however, there was variability in task success within the remaining sample. In future investigations, it may be more effective to employ parametric task manipulations, to equate performance across participants, and be able to define task difficulty on an individual subject basis. Nonetheless, findings from the current study provide evidence that brain function continues to be affected by HIV and comorbid factors, and also suggest that FMRI could provide a useful biomarker for assessing these effects. Additional research is needed to test the value of these FMRI metrics for predicting functional outcome in people living with chronic HIV infection.

Acknowledgments

References

Ances B, Vaida F, Ellis R, Buxton R. Test-retest stability of calibrated BOLD-fMRI in HIV- and HIV + subjects. NeuroImage. 2011; 54:2156–2162. doi: 10.1016/j.neuroimage.2010.09.081. [PubMed: 20932922]

Ances BM, Ortega M, Vaida F, et al. Independent effects of HIV, aging, and HAART on brain volumetric measures. J Acquir Immune Defic Syndr 1999. 2012; 59:469–477. doi: 10.1097/QAI. 0b013e318249db17.

Ances BM, Roc AC, Korczykowski M, et al. Combination antiretroviral therapy modulates the blood oxygen level-dependent amplitude in human immunodeficiency virus-seropositive patients. J Neurovirol. 2008; 14:418–424. doi: 10.1080/13550280802298112. [PubMed: 19040188]

Andersson, J.; Jenkinson, M.; Smith, SM. FMRIB technical report TR07JA2. Oxford: 2007. Non-linear registration, aka Spatial normalisation..

Andersson J, Smith SM. Non-linear optimisation. FMRIB technical report TR07JA1. Oxford. 2007

Becker JT, Maruca V, Kingsley LA, et al. Factors affecting brain structure in men with HIV disease in the post-HAART era. Neuroradiology. 2012; 54:113–121. doi: 10.1007/s00234-011-0854-2. [PubMed: 21424708]

Becker JT, Sanders J, Madsen SK, et al. Subcortical brain atrophy persists even in HAART-regulated HIV disease. Brain Imaging Behav. 2011; 5:77–85. doi: 10.1007/s11682-011-9113-8. [PubMed: 21264551]

Bullmore ET, Suckling J, Overmeyer S, et al. Global, voxel, and cluster tests, by theory and permutation, for a difference between two groups of structural MR images of the brain. IEEE Trans Med Imaging. 1999; 18:32–42. [PubMed: 10193695]

Burdo TH, Soulas C, Orzechowski K, et al. Increased monocyte turnover from bone marrow correlates with severity of SIV encephalitis and CD163 levels in plasma. PLoS Pathog. 2010; 6:e1000842. doi: 10.1371/journal.ppat.1000842. [PubMed: 20419144]

Chang L, Holt JL, Yakupov R, et al. Lower cognitive reserve in the aging human immunodeficiency virus-infected brain. Neurobiol Aging. 2013; 34:1240–1253. doi: 10.1016/j.neurobiolaging. 2012.10.012. [PubMed: 23158761]

Author Manuscript

Author Manuscript

Author Manuscript

Author Manuscript

Chang L, Speck O, Miller EN, et al. Neural correlates of attention and working memory deficits in HIV patients. Neurology. 2001; 57:1001–1007. [PubMed: 11571324]

Chang L, Tomasi D, Yakupov R, et al. Adaptation of the attention network in human immunodeficiency virus brain injury. Ann Neurol. 2004; 56:259–272. doi: 10.1002/ana.20190. [PubMed: 15293278]

Chang L, Yakupov R, Nakama H, et al. Antiretroviral treatment is associated with increased attentional load-dependent brain activation in HIV patients. J Neuroimmune Pharmacol Off J Soc NeuroImmune Pharmacol. 2008; 3:95–104. doi: 10.1007/s11481-007-9092-0.

Clark US, Cohen RA. Brain dysfunction in the era of combination antiretroviral therapy: implications for the treatment of the aging population of HIV-infected individuals. Curr Opin Investig Drugs 2000. 2010; 11:884–900.

Cohen RA, Harezlak J, Gongvatana A, et al. Cerebral metabolite abnormalities in human immunodeficiency virus are associated with cortical and subcortical volumes. J Neurovirol. 2010a; 16:435–444. doi: 10.3109/13550284.2010.520817. [PubMed: 20961212]

Cohen RA, Harezlak J, Schifitto G, et al. Effects of Nadir CD4 Count and Duration of HIV Infection on Brain Volumes in the HAART Era. J Neurovirol. 2010b; 16:25–32. doi: 10.3109/13550280903552420. [PubMed: 20113183]

Cohen RA, de la Monte S, Gongvatana A, et al. Plasma cytokine concentrations associated with HIV/ hepatitis C coinfection are related to attention, executive and psychomotor functioning. J Neuroimmunol. 2011; 233:204–210. doi: 10.1016/j.jneuroim.2010.11.006. [PubMed: 21146232]

Crum-Cianflone NF, Moore DJ, Letendre S, et al. Low prevalence of neurocognitive impairment in early diagnosed and managed HIV-infected persons. Neurology. 2013; 80:371–379. doi: 10.1212/ WNL.0b013e31827f0776. [PubMed: 23303852]

Devlin KN, Gongvatana A, Clark US, et al. Neurocognitive effects of HIV, hepatitis C, and substance use history. J Int Neuropsychol Soc JINS. 2012; 18:68–78. doi: 10.1017/S1355617711001408.

Ellis RJ, Badiee J, Vaida F, et al. CD4 nadir is a predictor of HIV neurocognitive impairment in the era of combination antiretroviral therapy. AIDS Lond Engl. 2011; 25:1747–1751. doi: 10.1097/QAD. 0b013e32834a40cd.

Ernst T, Chang L, Jovicich J, et al. Abnormal brain activation on functional MRI in cognitively asymptomatic HIV patients. Neurology. 2002; 59:1343–1349. [PubMed: 12427881]

Ernst T, Yakupov R, Nakama H, et al. Declined neural efficiency in cognitively stable human immunodeficiency virus patients. Ann Neurol. 2009; 65:316–325. doi: 10.1002/ana.21594. [PubMed: 19334060]

Forton DM, Allsop JM, Main J, et al. Evidence for a cerebral effect of the hepatitis C virus. Lancet. 2001; 358:38–39. doi: 10.1016/S0140-6736(00)05270-3. [PubMed: 11454379]

Fox MD, Zhang D, Snyder AZ, Raichle ME. The global signal and observed anticorrelated resting state brain networks. J Neurophysiol. 2009; 101:3270–3283. doi: 10.1152/jn.90777.2008. [PubMed: 19339462]

Garvey LJ, Pavese N, Ramlackhansingh A, et al. Acute HCV/HIV coinfection is associated with cognitive dysfunction and cerebral metabolite disturbance, but not increased microglial cell activation. PloS One. 2012; 7:e38980. doi: 10.1371/journal.pone.0038980. [PubMed: 22808022]

Gongvatana A, Harezlak J, Buchthal S, et al. Progressive cerebral injury in the setting of chronic HIV infection and antiretroviral therapy. J Neurovirol. 2013 doi: 10.1007/s13365-013-0162-1.

Gongvatana A, Schweinsburg BC, Taylor MJ, et al. White matter tract injury and cognitive impairment in human immunodeficiency virus-infected individuals. J Neurovirol. 2009; 15:187–195. doi: 10.1080/13550280902769756. [PubMed: 19306228]

Gusnard DA, Akbudak E, Shulman GL, Raichle ME. Medial prefrontal cortex and self-referential mental activity: relation to a default mode of brain function. Proc Natl Acad Sci U S A. 2001; 98:4259–4264. doi: 10.1073/pnas.071043098. [PubMed: 11259662]

Hayasaka S, Nichols TE. Combining voxel intensity and cluster extent with permutation test framework. NeuroImage. 2004; 23:54–63. doi: 10.1016/j.neuroimage.2004.04.035. [PubMed: 15325352]

Heaton RK, Clifford DB, Franklin DR Jr, et al. HIV-associated neurocognitive disorders persist in the era of potent antiretroviral therapy: CHARTER Study. Neurology. 2010; 75:2087–2096. doi: 10.1212/WNL.0b013e318200d727. [PubMed: 21135382]

Jenkinson M, Bannister P, Brady M, Smith S. Improved optimization for the robust and accurate linear registration and motion correction of brain images. NeuroImage. 2002; 17:825–841. [PubMed: 12377157]

Jenkinson M, Smith S. A global optimisation method for robust affine registration of brain images. Med Image Anal. 2001; 5:143–156. [PubMed: 11516708]

Jernigan TL, Archibald SL, Fennema-Notestine C, et al. Clinical factors related to brain structure in HIV: the CHARTER study. J Neurovirol. 2011; 17:248–257. doi: 10.1007/s13365-011-0032-7. [PubMed: 21544705]

Joska JA, Gouse H, Paul RH, et al. Does highly active antiretroviral therapy improve neurocognitive function? A systematic review. J Neurovirol. 2010; 16:101–114. doi: 10.3109/13550281003682513. [PubMed: 20345318]

Kim AY, Onofrey S, Church DR. An Epidemiologic Update on Hepatitis C Infection in Persons Living With or at Risk of HIV Infection. J Infect Dis. 2013; 207:S1–S6. doi: 10.1093/infdis/jis927. [PubMed: 23390299]

Letendre SL, Ellis RJ, Everall I, et al. Neurologic complications of HIV disease and their treatment. Top HIV Med. 2009; 17:46–56. [PubMed: 19401607]

Liner KJ 2nd, Ro MJ, Robertson KR. HIV, antiretroviral therapies, and the brain. Curr HIV/AIDS Rep. 2010; 7:85–91. doi: 10.1007/s11904-010-0042-8. [PubMed: 20425562]

Muller-Oehring EM, Schulte T, Rosenbloom MJ, et al. Callosal Degradation in HIV-1 Infection Predicts Hierarchical Perception: A DTI study. Neuropsychologia. 2010; 48:1133–1143. doi: 10.1016/j.neuropsychologia.2009.12.015. [PubMed: 20018201]

Nichols TE, Holmes AP. Nonparametric permutation tests for functional neuroimaging: a primer with examples. Hum Brain Mapp. 2002; 15:1–25. [PubMed: 11747097]

Oakes TR, Fox AS, Johnstone T, et al. Integrating VBM into the General Linear Model with voxelwise anatomical covariates. NeuroImage. 2007; 34:500–508. doi: 10.1016/j.neuroimage.2006.10.007. [PubMed: 17113790]

Owen AM, McMillan KM, Laird AR, Bullmore E. N-back working memory paradigm: a meta-analysis of normative functional neuroimaging studies. Hum Brain Mapp. 2005; 25:46–59. doi: 10.1002/hbm.20131. [PubMed: 15846822]

Penner I-K, Rausch M, Kappos L, et al. Analysis of impairment related functional architecture in MS patients during performance of different attention tasks. J Neurol. 2003; 250:461–472. doi: 10.1007/s00415-003-1025-0. [PubMed: 12700913]

Pfefferbaum A, Rosenbloom MJ, Sassoon SA, et al. Regional brain structural dysmorphology in human immunodeficiency virus infection: effects of acquired immune deficiency syndrome, alcoholism, and age. Biol Psychiatry. 2012; 72:361–370. doi: 10.1016/j.biopsych.2012.02.018. [PubMed: 22458948]

Ragin AB, Du H, Ochs R, et al. Structural brain alterations can be detected early in HIV infection. Neurology. 2012; 79:2328–2334. doi: 10.1212/WNL.0b013e318278b5b4. [PubMed: 23197750]

Raichle ME, MacLeod AM, Snyder AZ, et al. A default mode of brain function. Proc Natl Acad Sci U S A. 2001; 98:676–682. doi: 10.1073/pnas.98.2.676. [PubMed: 11209064]

Rempel H, Sun B, Calosing C, et al. Monocyte activation in HIV/HCV coinfection correlates with cognitive impairment. PloS One. 2013; 8:e55776. doi: 10.1371/journal.pone.0055776. [PubMed: 23437063]

Siemens Corporation. Germany Simmonds DJ, Fotedar SG, Suskauer SJ, et al. Functional brain correlates of response time variability in children. Neuropsychologia. 2013; 2007; 45:2147–2157. doi: 10.1016/j.neuropsychologia.2007.01.013.

Snodgrass JG, Corwin J. Pragmatics of measuring recognition memory: applications to dementia and amnesia. J Exp Psychol Gen. 1988; 117:34–50. [PubMed: 2966230]

Sun B, Abadjian L, Rempel H, et al. Peripheral biomarkers do not correlate with cognitive impairment in highly active antiretroviral therapy-treated subjects with human immunodeficiency virus type 1

infection. J Neurovirol. 2010; 16:115–124. doi: 10.3109/13550280903559789. [PubMed: 20307252]

Sun B, Abadjian L, Rempel H, et al. Differential cognitive impairment in HCV coinfected men with controlled HIV compared to HCV monoinfection. J Acquir Immune Defic Syndr 1999. 2013; 62:190–196. doi: 10.1097/QAI.0b013e31827b61f1.

Sweet LH, Rao SM, Primeau M, et al. Functional magnetic resonance imaging response to increased verbal working memory demands among patients with multiple sclerosis. Hum Brain Mapp. 2006; 27:28–36. doi: 10.1002/hbm.20163. [PubMed: 16001441]

Taylor MJ, Letendre SL, Schweinsburg BC, et al. Hepatitis C virus infection is associated with reduced white matter N-acetylaspartate in abstinent methamphetamine users. J Int Neuropsychol Soc. 2004; 10:110–113. doi: 10.1017/S1355617704101161. [PubMed: 14751013]

Thompson PM, Dutton RA, Hayashi KM, et al. Thinning of the cerebral cortex visualized in HIV/ AIDS reflects CD4+ T lymphocyte decline. Proc Natl Acad Sci U S A. 2005; 102:15647–15652. doi: 10.1073/pnas.0502548102. [PubMed: 16227428]

Tomasi D, Chang L, de Castro Caparelli E, et al. The human immunodeficiency virus reduces network capacity: acoustic noise effect. Ann Neurol. 2006; 59:419–423. doi: 10.1002/ana.20766. [PubMed: 16437575]

Towgood KJ, Pitkanen M, Kulasegaram R, et al. Mapping the brain in younger and older asymptomatic HIV-1 men: frontal volume changes in the absence of other cortical or diffusion tensor abnormalities. Cortex J Devoted Study Nerv Syst Behav. 2012; 48:230–241. doi: 10.1016/ j.cortex.2011.03.006.

Valcour VG, Shiramizu BT, Shikuma CM. HIV DNA in circulating monocytes as a mechanism to dementia and other HIV complications. J Leukoc Biol. 2010; 87:621–626. doi: 10.1189/jlb. 0809571. [PubMed: 20130221]

Wendelken LA, Valcour V. Impact of HIV and aging on neuropsychological function. J Neurovirol. 2012; 18:256–263. doi: 10.1007/s13365-012-0094-1. [PubMed: 22528478]

Winston A, Garvey L, Scotney E, et al. Does acute hepatitis C infection affect the central nervous system in HIV-1 infected individuals? J Viral Hepat. 2010; 17:419–426. doi: 10.1111/j. 1365-2893.2009.01198.x. [PubMed: 19780944]
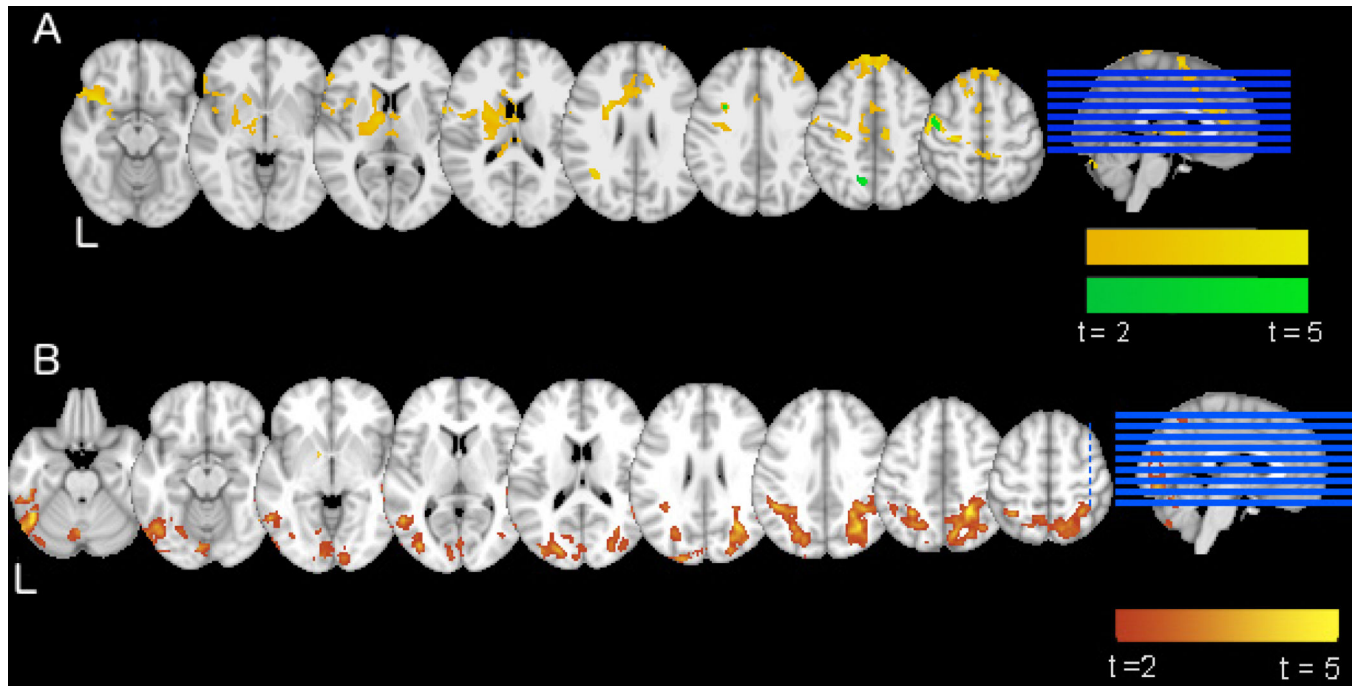
Fig. 1.
Illustration of between-group differences in neural activation to task. A) Greater 2-back vs. rest activation in HIV+ individuals with HCV coinfection, as compared to HIV-seronegative participants (yellow) and HIV+ participants (green). Colors range from t = 2 to t = 5 for both contrasts. Axial slices begin at z = 20. B) Greater 2-back vs. 0-back activation in HIV-seronegative vs. HIV+ participants. Colors range from t = 2 (red) to t = 5 (yellow). Axial slices begin at z = 25

Author Manuscript

Author Manuscript

Author Manuscript

Author Manuscript

Table 1

Group characteristics.

Characteristic	Full Sample (n=62)	HIV- (n=28)	HIV+ (n=26)	HIV/HCV+ (n=8)	p
Age (years)	45.29 (10.7)	44.9 (12.7)	45.1 (9.4)	47.1 (7.5)	ns[a]
Education (years)	13.45 (2.8)	14.0 (3.4)	13.3 (2.0)	11.9 (1.5)	0.097[a]
Proportion male (%)	61	54	61	88	ns[a]
Proportion Caucasian (%)	66	68	69	50	ns[a]
Time since HIV diagnosis (years)	N/A	N/A	13.6 (7.0)	14.5 (8.0)	ns[b]
CD4 nadir (cells/ml)	N/A	N/A	213.7 (174.5)	161.2 (136.4)	ns[b]
Current CD4 (cells/ml)	N/A	N/A	575.9 (309.9)	467.6 (240.4)	ns[b]
Proportion undetectable HIV RNA (viral load) (%)	N/A	N/A	73	75	ns[b]
Proportion on cART (%)	N/A	N/A	81	75	ns[b]

Note. cART, Combination Antiretroviral Therapy; ns, nonsignificant. Continuous variables are represented as mean (SD).

[a] Kruskall-Wallace tests comparing HIV seronegative, HIV+, and HIV/HCV seropositive groups on demographic measures.

[b] Mann-Whitney tests comparing HIV+ and HIV/HCV seropositive groups on clinical measures.

Table 2

N-back task performance.

Measure	Full Sample (n=62)	HIV- (n=28)	HIV+ (n=26)	HIV/HCV+ (n=8)	p
0-Back reaction time (ms)	626.8 (138.4)	587.6 (140.7)	668.1 (139.3)	634.5 (94.9)	0.031 [a]
0-Back reaction time variability	.4987 (.022)	.4960 (.013)	.4964 (.018)	.5159 (.046)	ns [a]
0-Back performance (A')	.9784 (.029)	.9875 (.012)	.9667 (.040)	.9844 (.010)	ns [a]
0-Back bias (B')	-.0259 (.241)	-.0418 (.213)	-.0286 (.236)	.0385 (.355)	ns [a]
2-Back reaction time (ms)	945.3 (298.9)	841.5 (275.7)	1054.5 (285.7)	967.3 (326.2)	0.013 [a]
2-Back reaction time variability	.3557 (.098)	.3611 (.113)	.3471 (.077)	.3639 (.116)	ns [a]
2-Back performance (A')	.8336 (.109)	.8700 (.075)	.7977 (.138)	.8229 (.064)	ns [a]
2-Back bias (B')	.0524 (.221)	.0653 (.228)	-.0098 (.221)	.2090 (.093)	0.023 [a]

Note. ns, nonsignificant. Variables are represented as mean (SD).

[a] Kruskall-Wallace tests comparing HIV seronegative, HIV+, and HIV/HCV seropositive groups on each performance measure.

Table 3

Significant FMRI activation by task condition and diagnostic group.

	Primary Regions	Size (Voxels)	Max T-Statistic	MNI-Coordinates of Peak (x, y, z)
0-Back				
HIV-Seronegative [a]				
	Bilateral SMA	230	8.77	−6, 0, 50
	Right cerebellum	285	7.1	26, −52, 30
	Left occipital/cerebellum	412	8.19	−40, −86, −10
	Right occipital/cerebellum	508	8.61	46, −80, −6
	Left parietal/motor	2469	11.5	−40, −18, 56
HIV-Seropositive [a]				
	Bilateral SMA	405	9.59	6, 6, 46
	Left parietal/motor	2852	11.9	−38, −18, 58
	Bilateral occipital/cerebellum	7117	10.5	26, −52, −28
HIV/HCV Coinfected [a]				
	Right precentral	10	7.99	40, −10, 58
	Right superior parietal	20	7.07	34, −52, 44
	Left parietal/motor, bilateral SMA	3122	9.51	−40, −20, 58
	Bilateral cerebellum	7789	7.46	−34, −68, −30
2-Back				
HIV-Seronegative [b]				
	Right superior temporal	20	8.22	54, −48, −18
	Left cerebellum	293	9.63	−10, −76, −30
	Right cerebellum	301	10.6	8, −76, −26
	Right cerebellum/occipital	713	10.1	30, −60, −34
	Left cerebellum/occipital	866	10.6	−36, −68, −30
	Bilateral frontal/SMA/parietal	19198	15	36, −54, 40
HIV-Seropositive [b]				
	Left cerebellum	248	8.24	−10, −76, −32
	Right insula	692	10.3	38, 20, −2
	Left cerebellum	736	10.9	−38, −68, −30
	Right parietal	1039	13.1	36, −54, 40
	Right cerebellum	1230	10.8	8, −76, −28
	Right frontal/BG	5336	10	44, 28, 26
	Bilateral SMA; Left frontal, parietal	12550	11.3	−30, −58, 44
HIV/HCV Coinfected [b]				
	Left occipital	32	7.41	−32, −86, −6
	Left inferior temporal	44	6.21	−44, −64, −14
	Bilateral cerebellum	2164	11.4	−36, −68, −30
	Bilateral frontal/SMA/parietal/BG	19155	10.5	42, −8, 54

	Primary Regions	Size (Voxels)	Max T-Statistic	MNI-Coordinates of Peak (x, y, z)
2-Back > 0-Back				
HIV-Seronegative [a]				
	Right inferior temporal	603	9.01	54, −48, −18
	Bilateral cerebellum	5072	12	34, −56, −38
	Bilateral parietal	10377	15.2	34, −64, 42
	Bilateral frontal/SMA	28548	12.2	44, 26, 28
HIV-Seropositive [a]				
	Left cerebellum	10	8.04	−30, −62, −34
	Right cerebellum	93	8.94	32, −60, −36
	Right cerebellum	160	9.8	10, −76, −30
	Bilateral precuneus	558	6.91	2, −68, 46
	Right parietal	1160	9.53	38, −54, 38
	Left parietal	1410	9.61	−34, −56, 40
	Bilateral frontal/SMA/BG	23107	10.1	−32, 20, −8
HIV/HCV Coinfected [c]				
	Bilateral precuneus	935	6.66	−8, −64, 40
	Left parietal	973	6.34	−26, −56, 52
	Right parietal	1520	8.14	42, −46, 34
	Bilateral frontal/SMA/BG	16015	8.03	−34, 18, −8

Note. BG, Basal Ganglia; SMA, Supplementary Motor Area. All regions presented show significant activation for the indicated task condition (i.e., 0-back, 2-back, and 2-back > 0-back), separately for each clinical group (i.e., HIV+, HIV-seronegative, and HIV/HCV coinfected). Exact significance levels are presented for each analysis; these reflect the exact criteria for each group and condition, and are impacted by contrast type and sample size (i.e., group size). Coordinates represent peak activation voxel. Between-group differences are presented in Table 4.

[a] Family-wise p = 0.99; Voxel-wise p = 0.0001

[b] Family-wise p = 0.9998, Voxel-wise p = 0.0000001

[c] Family-wise p = 0.999, Voxel-wise p = 0.0001

Table 4

Between-Groups Activation Differences, by Task Condition.

	Primary Regions	Size (Voxels)	Max T-Statistic	MNI-Coordinates of Peak (x, y, z)
0-Back				
HIV/HCV Coinfected > HIV Seronegative [a]				
	Left occipital	7	3.92	−32, −86, −4
	Left occipital	8	3.94	−26, −82, 0
	Right cerebellum	88	4.19	10, −58, −50
	Bilateral cerebellum	1315	5.53	−34, −70, −30
2-Back				
HIV/HCV Coinfected > HIV Seronegative [a]				
	Right postcentral	20	3.32	6, −40, 64
	Right angular gyrus	65	4.2	40, −52, 26
	Left SMA	99	3.99	−8, −20, 48
	Bilateral cerebellum	345	5.75	−36, −70, −30
	Bilateral precentral	1546	8.35	44, −8, 56
	Bilateral frontal; left insula/BG	6105	4.63	−2, 44, 44
HIV/HCV Coinfected > HIV Seropositive [a]				
	Right frontal	12	5.1	30, 8, 36
	Right cerebellum	20	5.22	18, −84, −28
	Right precentral	42	7.79	42, −8, 54
	Right precuneus/occipital	46	5.64	10, −60, 46
	Left cerebellum	89	5.76	−36, −72, −30
2-Back > 0-Back				
HIV Seronegative > HIV Seropositive [a]				
	Left thalamus/BG	14	4.53	−12, 2, −4
	Right inferior temporal	38	3.84	54, −48, −20
	Bilateral parietal; left occipital/cerebellum	10975	5.28	28, −64, 30

Note. BG, Basal Ganglia; SMA, Supplementary Motor Area. All regions presented show significant between-group comparisons for clinical groups (i.e., HIV+, HIV-seronegative, and HIV/HCV coinfected), by task condition (i.e., 0-back, 2-back, and 2-back > 0-back). Exact significance levels are presented for each analysis; these are impacted by contrast type and sample size (i.e., group size). Coordinates represent peak activation voxel.

[a] Family-wise p = 0.95; Voxel-wise p = 0.001

Table 5

Correlation of FMRI Activation to Clinical Factors, by Task and Diagnostic Group.

	Primary Regions	Size (Voxels)	Max Z-Statistic	MNI-Coordinates of Center of Gravity (x, y, z)
Time Since HIV Diagnosis				
0-Back				
HIV-Seropositive, Positive Correlation [a]	Bilateral precuneus/posterior cingulate	2957	4.28	8, −45, 52
	Bilateral occipital; right temporal/frontal	5079	4.65	22, −49, −4
HIV-Seropositive, Negative Correlation [b]	Bilateral BG	1229	3.28	0, −7, 11
HIV/HCV Coinfected, Positive Correlation [c]	Right hippocampus/temporal	1218	3.01	29, −5, −36
2-Back				
HIV-Seropositive, Positive Correlation [d]	Right Lateral/Occipital	254	4.22	43, −66, 8
	Bilateral Occipital; Right Precuneus	541	4.91	5, −68, 17
2-Back > 0-Back				
HIV/HCV Coinfected, Positive Correlation [a]	Right frontal/BG	2974	3.5	26, 24, 17
	Bilateral frontal/central/superior parietal; left BG	6089	3.52	−17, 1, 35

	Primary Regions	Size (Voxels)	Max Z-Statistic	MNI-Coordinates of Center of Gravity (x, y, z)
CD4 Nadir				
0-Back				
HIV-Seropositive, Positive Correlation [c]	Bilateral occipital; right cerebellar/parietal	4368	4.38	21, −71, −4
	Right lateral and dorsolateral frontal, motor	5154	5.26	33, 34, 20
HIV-Seropositive, Negative Correlation [c]	Bilateral posterior cingulate	1421	4.58	0, −54, 31
HIV/HCV Coinfected, Positive Correlation [c]	Bilateral ACC/medial frontal	1377	3.13	6, 42, 6
HIV/HCV Coinfected, Negative Correlation [a]	Bilateral occipital/cerebellar/thalamic	8576	3.46	8, −56, −14
2-Back				
HIV-Seropositive, Positive Correlation [e]	Right middle/inferior frontal	323	4.85	42, 11, 20
	Bilateral cerebellum/occipital	749	4.69	6, −61, −14
HIV/HCV Coinfected, Positive Correlation [d]	Left parietal	1753	3.42	−43, −41, 48
	Right insula/inferior frontal/temporal pole	2358	3.42	49, −15, 22
	Bilateral superior/medial frontal/ACC	3124	3.74	4, 39, 30

	Primary Regions	Size (Voxels)	Max Z-Statistic	MNI-Coordinates of Center of Gravity (x, y, z)
HIV/HCV Coinfected, Negative Correlation [d]	Bilateral cerebellum	1695	3.18	1, −43, −36
	Bilateral BG/temporal/parietal/occipital	9445	3.32	−8, −48, 13
2-Back > 0-Back				
HIV-Seropositive, Positive Correlation [a]	Bilateral SMA; right parietal	2494	5.35	0, −1, 40
HIV/HCV Coinfected, Positive Correlation [c]	Left frontal	1327	3.22	32, 52, 12
HIV/HCV Coinfected, Negative Correlation [a]	Left central/parietal/occipital	2777	3.06	−27, −23, 24

	Primary Regions	Size (Voxels)	Max Z-Statistic	MNI-Coordinates of Center of Gravity (x, y, z)
CD4 Count				
0-Back				
HIV-Seropositive, Positive Correlation [f]	Right orbitofrontal	532	4.6	14, 40, −21
HIV-Seropositive, Negative Correlation [a]	Bilateral ACC/medial frontal	5800	4.92	28, −6, 32
HIV/HCV Coinfected Positive Correlation [c]	Left middle/superior temporal	1211	3.09	−58, −22, −5
	Bilateral ACC; right frontal	1588	3.02	12, 39, 0
HIV/HCV Coinfected Negative Correlation [f]	Right occipital	466	3.6	28, −93, 4
2-Back				
HIV-Seropositive, Negative Correlation [b]	Right pre/post-central	230	5.15	51, −14, 47
HIV/HCV Coinfected Positive Correlation [g]	Right ACC	374	3.88	14, 40, 9
HIV/HCV Coinfected Negative Correlation [c]	Right occipital	1447	3.71	29, −93, 4
	Bilateral BG; left inferior frontal	1789	3.05	3, −20, 7
2-Back > 0-Back				
HIV-Seropositive, Negative Correlation [e]	Bilateral occipital	324	4.47	9, −82, 26
	Bilateral post-central/precuneus	506	4.01	4, −35, 56
HIV/HCV Coinfected, Positive Correlation [a]	Right frontal	3150	3.41	30, 32, 31

Note. ACC, Anterior Cingulate Cortex; BG, Basal Ganglia; SMA, Supplementary Motor Area. Clusters of significant correlation between neural activation to 0-back, 2-back, and 2-back > 0-back task conditions and clinical factors (i.e., time since HIV diagnosis, CD4 Nadir, and CD4 Count) within each diagnostic group (i.e., HIV+, HIV-seronegative, and HIV/HCV coinfected). Positive and negative correlations are listed separately. All regions presented show significant activation for the indicated group and condition. Exact significance levels are presented for each analysis. Coordinates represent center of gravity of clusters (i.e., weighted average of activation).

[a] Cluster z = 1.699; Family-wise p = 0.001

[b] Cluster z = 2.755; Family-wise p = 0.05

[c] Cluster z = 1.699; Family-wise p = 0.05

[d]Cluster z = 1.699; Family-wise p = 0.01

[e]Cluster z = 2.464; Family-wise p = 0.05

[f]Cluster z = 2.464; Family-wise p = 0.01

[g]Cluster z = 2.755; Family-wise p = 0.01

Table 6

Relationship of FMRI Activation to Viral Load Detectability.

	Primary Regions	Size (Voxels)	Max Z-Statistic	MNI-Coordinates of Peak (x, y, z)
Detectable >Undetectable				
0-Back[a]	Bilateral cerebellum/occipital	2205	3.75	−8, −84, 8
2-Back[a]	Bilateral frontal, precuneus, posterior cingulate	8264	0.358	−38, 28, 26
	Bilateral orbitofrontal; left temporal/BG	2127	3.92	−16, 4, −24
	Bilateral precuneus, posterior cingulate, ACC	7627	3.98	−22, −72, 46
2-Back > 0-Back [b]				
	Bilateral OFC, subgenual cingulate, temporal; left occipital	5741	3.33	−48, 12, −16
Undetectable > Detectable				
0-Back [c]				
	Left superior parietal/postcentral	1261	3.35	−36, −24, 64
2-Back[c]				
	Left superior parietal/lateral occipital	1809	4.62	−28, −64, 66
2-Back > 0-Back [c]				
	Diffuse; right ACC, superior frontal; left frontal	6004	4.14	−4, 28, 62

Note. ACC, Anterior Cingulate Cortex; OFC, Orbitofrontal Cortex; BG, Basal Ganglia. Clusters of significant correlation between neural activation to 0-back, 2-back, and 2-back > 0-back task conditions and current plasma viral load detectability, within each diagnostic group (HIV+, HIV-seronegative, and HIV/HCV coinfected). Positive and negative correlations are listed separately. All regions presented show significant activation for the indicated group and condition. Exact significance levels are presented for each analysis. Coordinates represent peak activation voxel.

[a]Cluster z = 1.699, Family-wise p = 0.001

[b]Cluster z = 1.699, Family-wise p = 0.0001

[c]Cluster z = 1.699, Family-wise p = 0.005